

An effective quasi-one-dimensional description of a spin-1 atomic condensate

Wenxian Zhang and L. You

School of Physics, Georgia Institute of Technology, Atlanta GA 30332-0430, USA

(Dated: March 23, 2022)

Within the mean field theory we extend the effective quasi-one-dimensional nonpolynomial Schrödinger equation (NPSE) approach to the description of a spin-1 atomic condensate in a tight radial confinement geometry for both weak and strong atom-atom interactions. Detailed comparisons with full time dependent 3D numerical simulations show excellent agreement as in the case of a single component scalar condensate, demonstrating our result as an efficient and effective tool for the understanding of spin-1 condensate dynamics observed in several recent experiments.

PACS numbers: 03.75.Mn, 03.75.Kk, 51.10.+y

Keywords: Spin-1 BEC, Quasi-1D BEC

Although our ability to perform numerical simulations keeps increasing with computer technology, full 3D time dependent calculations still represent a significant challenge. In many situations, one explores the inherent system symmetries, e.g., cylindrical and spherical symmetries in space, to reduce the number of spatial dimension from 3D to 2D or even 1D. The description of atomic condensate dynamics in terms of a mean field theory is such an example. With a tight radial confinement, a condensate becomes cigar-shaped. Several effective 1D approaches have been developed [1, 2, 3], with the simplest of them assuming a fixed transverse Gaussian profile. Recent studies, however, have indicated that the effective quasi-one-dimensional (1D) nonpolynomial Schrödinger equation (NPSE) is the most powerful and efficient tool, at least for a weakly interacting atomic condensate [1]. In this brief report, we generalize such an NPSE approach to the case of a spin-1 atomic condensate in a cigar-shaped trap.

Multi-component atomic condensates or spinor condensates have become an actively investigated topic in atomic quantum gases [4, 5, 6, 7, 8, 9, 10, 11, 12, 13, 14, 15, 16, 17]. The examples that have been experimentally realized include that of two-component pseudo-spin-1/2 [4], three-component spin-1, and five-component spin-2 condensates [5, 6, 9, 11]. Several recent experiments have observed interesting coherent spatial fragmentation of the spin-1 condensate when it is confined in a single running wave optical trap, i.e., in a cigar-shaped trap. To provide a proper theoretical description for these observations, numerical approaches have been used to study the nonlinear spatial-temporal dynamics for a spin-1 condensate. It is therefore desirable to have a more efficient theoretical approach instead of the 3D coupled Gross-Pitaevskii (GP) equations that is uniformly valid to both strongly and weakly interacting limits.

A spin-1 Bose condensate is described by the Hamiltonian in second quantized form (repeated indices are summed) as [12]

$$\hat{H} = \int d\mathbf{r} \sum_i \left[\frac{\hbar^2}{2M} \nabla^2 + V_{\text{ext}} + E_i \right] \hat{\psi}_i + \frac{C_0}{2} \sum_{i,j} \hat{\psi}_i^\dagger \hat{\psi}_j^\dagger \hat{\psi}_j \hat{\psi}_i + \frac{C_2}{2} \sum_{k,i} \hat{\mathbf{F}}_i \cdot \hat{\mathbf{F}}_k \hat{\psi}_i^\dagger \hat{\psi}_k \hat{\psi}_i \hat{\psi}_k^\dagger; \quad (1)$$

where $\hat{\psi}_j(\mathbf{r})$ ($\hat{\psi}_j^\dagger$) is the field operator that annihilates (creates) an atom in the j th internal state at location \mathbf{r} , $j = +; 0; -$ denotes atomic hyperfine state $F = 1; m_F = +1; 0; -1$, respectively. M is the mass of each atom and $V_{\text{ext}}(\mathbf{r})$ is an internal-state-independent trap potential. Terms with coefficients C_0 and C_2 of Eq. (1) describe elastic collisions of two spin-1 atoms, expressed in terms of the scattering lengths a_0 (a_2) in the combined symmetric channel of total spin 0 (2), $C_0 = 4\hbar^2(a_0 + 2a_2)/3M$ and $C_2 = 4\hbar^2(a_2 - a_0)/3M$. $\mathbf{F} = x, y, z$ are spin-1 matrices [17]. Since an external magnetic field is usually present in experiments, it is also included in our formulation. For simplicity, the magnetic field B is taken along the quantization axis (\hat{z}). The Zeeman shift on each atomic state is then given by the Breit-Rabi formula [18].

Adopting the mean field theory when the condensate consists of a large number of atoms, we introduce the condensate order parameter or wave function $\psi_i = \langle \hat{\psi}_i \rangle$ for the i th component. Neglecting quantum fluctuations we arrive at the mean field energy functional,

$$E = \int d\mathbf{r} \sum_i \left[\frac{\hbar^2}{2M} \nabla^2 + V_{\text{ext}} + E_i \right] \psi_i + \frac{C_0}{2} \sum_{i,j} \psi_i^\dagger \psi_j^\dagger \psi_j \psi_i + \frac{C_2}{2} \sum_{k,i} \mathbf{F}_i \cdot \mathbf{F}_k \psi_i^\dagger \psi_k \psi_i \psi_k^\dagger; \quad (2)$$

from which the coupled GP equations can be derived according to $i\hbar \partial_t \psi_i = \delta E / \delta \psi_i^\dagger$. They are given below in explicit form as

$$i\hbar \frac{\partial}{\partial t} \psi_i + \left[\frac{\hbar^2}{2M} \nabla^2 + V_{\text{ext}} + E_i + C_0 n + C_2 (n_+ + n_0 - n_-) \right] \psi_i = 0; \quad ;$$

$$\begin{aligned} i\hbar \frac{\partial}{\partial t} \psi_0 &= \frac{\hbar^2}{2M} \nabla^2 \psi_0 + V_{\text{ext}} + E_0 + c_0 n + c_2 (n_+ + n_-) \psi_0 + 2c_2 \psi_+ \psi_-; \\ i\hbar \frac{\partial}{\partial t} \psi_{\pm} &= \frac{\hbar^2}{2M} \nabla^2 \psi_{\pm} + V_{\text{ext}} + E_{\pm} + c_0 n + c_2 (n_+ + n_0 - n_{\mp}) \psi_{\pm} + c_2 \psi_0^2 \psi_{\pm}; \end{aligned} \quad (3)$$

where $n = \sum_i n_i$ is the total condensate density and $n_i = \int |\psi_i|^2$.

The external trap is assumed harmonic $V_{\text{ext}} = M(\frac{1}{2}r_{\perp}^2 + \frac{1}{2}z^2) = 2$ with cylindrical symmetry $\psi_x = \psi_y = \psi_{\perp}$, and $\psi_z = \psi_{\parallel}$, i.e., cigar shaped. Following the successful approach of the NPSE description as for a single component scalar condensate [1], we factor the wave function into transversal and longitudinal functions as

$$\psi_i(\mathbf{r}; z; t) = \frac{1}{N_{\perp}} \psi_{\perp}(\mathbf{r}; z; t) f_i(z; t); \quad (4)$$

where ψ_{\perp} and f_i are variational functions which depend on z and t . ψ_{\perp} is the transversal wave function, satisfying $\int d\mathbf{r}_{\perp} |\psi_{\perp}|^2 = 1$, and is assumed identical for all components. Substituting Eq. (4) into Eq. (3), we obtain the Lagrangian of our system as

$$\begin{aligned} L &= \int d\mathbf{r}_{\perp} \int dz \left[\sum_i \left(\frac{1}{2} \dot{\psi}_i^2 + \frac{\hbar^2}{2M} \nabla_{\perp}^2 \psi_i^2 - V_{\text{ext}} \psi_i^2 - E_i \psi_i^2 - \frac{c_0 N}{2} \sum_j |\psi_j|^2 \psi_i^2 - \frac{c_2 N}{2} \sum_j |\psi_j|^4 \right) \right. \\ &\quad \left. + \sum_i \left(\frac{1}{2} \dot{f}_i^2 + \frac{\hbar^2}{2M} \frac{\partial^2}{\partial z^2} f_i^2 - V(z) f_i^2 - E_{\parallel} f_i^2 - E_{\perp} f_i^2 - \left(\frac{c_0 N}{2} \right) f_i^2 \sum_j |\psi_j|^2 - \left(\frac{c_2 N}{2} S_2 \right) f_i^4 \right) \right] \end{aligned} \quad (5)$$

where $V(z) = M \frac{1}{2} z^2 = 2$. E_{\perp} is the transverse mode energy, and $E_{\parallel}(z) = \int d\mathbf{r}_{\perp} \left[\frac{\hbar^2}{2M} \nabla_{\perp}^2 \psi_{\perp}^2 + M \frac{1}{2} r_{\perp}^2 \psi_{\perp}^2 \right]$. γ is the scaling factor of the nonlinear interaction strength, $\gamma(z) = \int d\mathbf{r}_{\perp} |\psi_{\perp}|^4$, $\psi_{\perp}(z) = \int d\mathbf{r}_{\perp} |\psi_{\perp}|^2$, and S_2 is independent of z and given by

$$S_2 = \int d\mathbf{r}_{\perp} |\psi_{\perp}|^4 + \int d\mathbf{r}_{\perp} |\psi_{\perp}|^4 + 2 \int d\mathbf{r}_{\perp} |\psi_{\perp}|^2 |\psi_0|^2 + 2 \int d\mathbf{r}_{\perp} |\psi_{\perp}|^2 |\psi_0|^2 - 2 \int d\mathbf{r}_{\perp} |\psi_{\perp}|^2 |\psi_{\perp}|^2 + 2 f_0^2 f_+ f_- + 2 f_+ f_- f_0^2;$$

To obtain the above result, we have also assumed a weak time and z dependence of the transverse wave function, i.e., $\partial_t \psi_{\perp} = \partial_t' \psi_{\perp}$ and $r_{\perp}^2 \psi_{\perp}' = r_{\perp}^2 \psi_{\perp}$. The effective quasi-1D NPSE for a spin-1 condensate can now be derived from the least action principle of the above Lagrangian,

$$\begin{aligned} i\hbar \frac{\partial}{\partial t} f_+ &= \frac{\hbar^2}{2M} \frac{\partial^2}{\partial z^2} f_+ + V(z) f_+ + E_+ + E_{\perp} + c_0 N \sum_i f_i^2 + \gamma N (f_+ + f_0) f_+ + c_2 N f_0^2 f_+; \\ i\hbar \frac{\partial}{\partial t} f_0 &= \frac{\hbar^2}{2M} \frac{\partial^2}{\partial z^2} f_0 + V(z) f_0 + E_0 + E_{\perp} + c_0 N \sum_i f_i^2 + \gamma N (f_+ + f_-) f_0 + 2c_2 N f_+ f_- f_0; \\ i\hbar \frac{\partial}{\partial t} f_- &= \frac{\hbar^2}{2M} \frac{\partial^2}{\partial z^2} f_- + V(z) f_- + E_- + E_{\perp} + c_0 N \sum_i f_i^2 + \gamma N (f_+ + f_0) f_- + c_2 N f_0^2 f_-; \\ \frac{\partial E_{\perp}}{\partial \gamma} + \frac{c_0 N}{2} \sum_i f_i^2 + \frac{c_2 N}{2} S_2 \frac{\partial}{\partial \gamma} &= 0; \end{aligned} \quad (6)$$

where $n = \sum_i n_i$ is the total density and $n_i = \int |\psi_i|^2$ is the density of the i th component.

We discuss two separate ansatzes for the transverse function applicable respectively for the cases of weak and strong atomic interactions.

A Gaussian ansatz

For weak atomic interaction when $E_{\perp} \ll \hbar \omega_{\perp}$ is satisfied, the transverse wave function can be taken as a Gaussian function of a variable width,

$$\psi_{\perp}(\mathbf{r}_{\perp}; z; t) = \frac{1}{\sqrt{1+2}} \exp[-\frac{r_{\perp}^2}{2(1+2)}]; \quad (7)$$

The transverse mode energy and scaling factor are then given by

$$E_{\perp} = \frac{\hbar \omega_{\perp}}{2} \frac{a_{\perp}^2}{2} + \frac{1}{a_{\perp}^2}; \quad (8)$$

$$\gamma = \frac{1}{2(1+2)}; \quad (9)$$

where $a_{\perp} = \frac{1}{\hbar M \omega_{\perp}}$.

A Thomas-Fermi ansatz

For strong atomic interactions when $E_{\perp} \gg \hbar \omega_{\perp}$ holds, the transverse wave function is taken as a Thomas-Fermi (TF) ansatz,

$$\psi_{\perp}(r; z; t) = \begin{cases} \frac{1}{\sqrt{2}} \left(\frac{r}{a_{\perp}} \right)^{-1/2} & r \leq a_{\perp} \\ 0 & r > a_{\perp} \end{cases} \quad (10)$$

The kinetic energy in the transverse direction is neglected, leading to the transverse mode energy and scaling factor as

$$E_{\perp} = \frac{\hbar \omega_{\perp}}{6} \frac{a_{\perp}^2}{a_z^2}; \quad (11)$$

$$= \frac{4}{3} \frac{\hbar \omega_{\perp}}{2}; \quad (12)$$

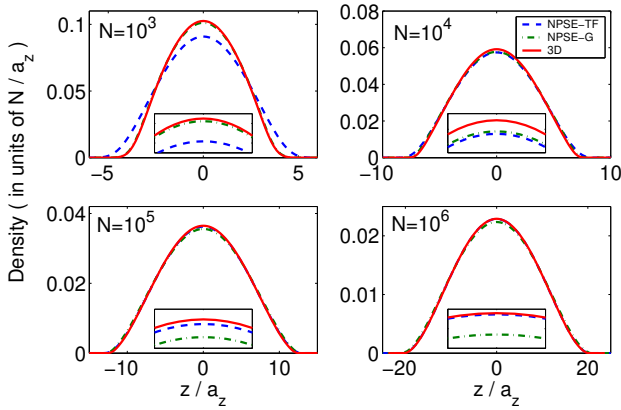


FIG. 1: The ground state density distribution of the condensate component in state $|j=1\rangle$ along the axis of the cigar-shaped trap, for ^{87}Rb atoms and without an external magnetic field ($a_z = \hbar/M \omega_z$). The inset shows the zoom-in central region. The solid line denotes the "exact", while the dashed and dash-dot lines denote respectively the results from our NPSE with a TF or a Gaussian ansatz for the transverse profile.

We performed some numerical simulations to illustrate the efficiency and effectiveness of the NPSE as developed by us for a spin-1 condensate in a cigar-shaped trap. For the first example, we computed the ground state of a ^{87}Rb spin-1 condensate by propagating the GP equations and the effective 1D NPSE with an imaginary time. The atomic parameters of ^{87}Rb are $a_0 = 101.8 a_B$ and $a_2 = 100.4 a_B$ [19]. The trap frequencies are $\omega_z = (2\pi)240$ Hz and $\omega_{\perp} = (2\pi)24$ Hz. The "exact" solution as given by the ground state of the full 3D coupled GP equations (3) is calibrated by its effective 1D distribution according to $\int |\psi(z)|^2 dz = \int |\psi_{\perp}(z)|^2 dz$. Figure 1 illustrates the results for several cases of different total number of atoms, N . We note that with increasing N , the mean field interaction becomes stronger. For weak interactions the quasi-1D NPSE with a Gaussian variational ansatz gives a better

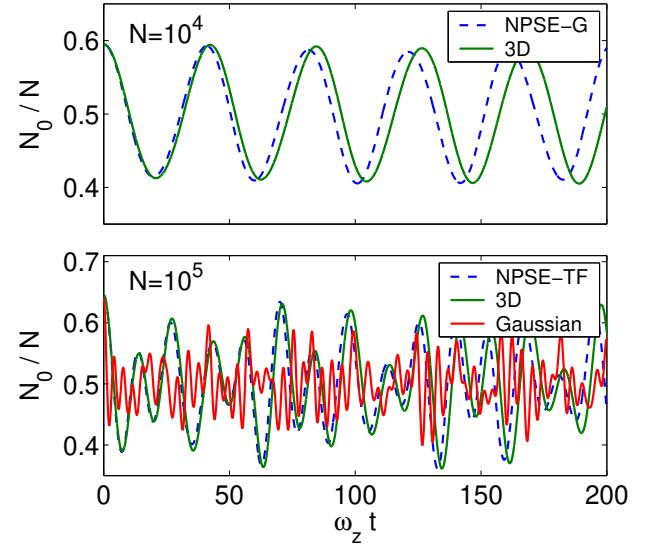


FIG. 2: The time dependence of the fractional condensate population in the $|j=1\rangle$ state N_0/N . The thick solid curve denotes the full 3D simulation while the dashed curve denotes the simulation with our effective quasi-1D NPSE. We have used $N = 10^4$ for the top part and $N = 10^5$ for the bottom. As a comparison we also presented the result obtained from a time-independent Gaussian ansatz (thin solid curve in the bottom panel), which is shown to give a poor agreement in the strong interaction regime.

result, while for strong interactions the quasi-1D NPSE with a TF ansatz is a better choice. Here "better" means the result obtained from an NPSE is closer to that of the full 3D solution. We also observe that the quasi-1D NPSE with a TF ansatz gives a lower central density and overestimates the TF radius in the weak interaction regime, while the quasi-1D NPSE with a Gaussian ansatz gives a lower central density and a correspondingly larger width in the strong interaction regime. Overall, it is interesting to point out that the quasi-1D NPSE with a Gaussian ansatz is not too bad even in the strong interaction regime.

To test the quasi-1D NPSE more strictly we study the dynamics of a spin-1 condensate out of equilibrium configuration and compare the results with those from a full 3D simulation with the coupled GP equations (3). The initial state is taken as the ground state in a given magnetic field. The simulation starts after the magnetic field is set zero, and we follow the spatial-temporal dynamics. With our NPSE, it becomes essentially a trivial task, and we find that excellent agreements are obtained with a Gaussian ansatz, e.g., with $N = 10^3$ atoms for weak interactions, and a TF ansatz for strong interactions with $N = 10^6$ atoms. In the results to be given below, we instead use the effective quasi-1D NPSE to simulate the dynamics in the limit between the strong and weak interactions, i.e., for $\hbar \omega_{\perp} \sim \hbar \omega_z$. For the quasi-1D NPSE approach, we use a Gaussian ansatz with $N = 10^4$ atoms ($E_{\perp} \sim \hbar \omega_{\perp} = 1.74 \hbar \omega_z$) and a TF ansatz with $N = 10^5$

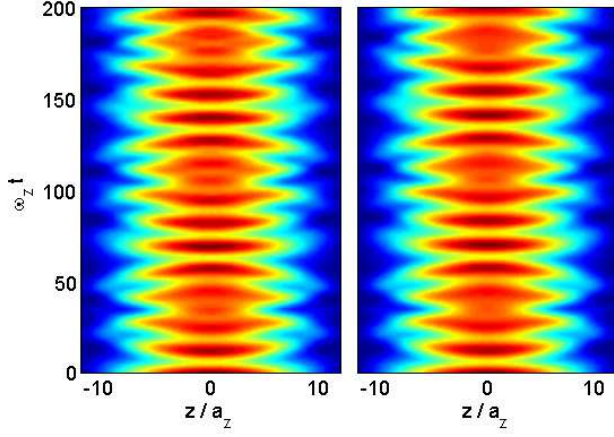


FIG. 3: The contour plots of the density of the j_1 component with respect to time and z . The left one is from the quasi-1D NPSE while the right one is the "exact" result from a full 3D simulation. Parameters are the same as Fig. 2.

atoms ($E_{\text{th}} = 4.98 h^2$). Figure 2 displays the time evolution of the fractional condensate in the j_1 state. For weak interactions, all three components share the space profile along the z axis, and the out of equilibrium dynamics is periodic [15, 16, 20]. Figure 2 also clearly shows the periodic motion for $N = 10^4$ atoms, although we do find that the quasi-1D NPSE gives a slightly shorter period than that of the full 3D simulation. For strong interactions, the apparent spatial profiles of the three spin components clearly become different, and the out of equilibrium dynamics also becomes complicated. Yet still, the quasi-1D NPSE simulations give results very close to the "exact" 3D solution, especially in the short time range. Figure 3 compares the dependence of the density distribution of the j_1 state component on time and space from quasi-1D NPSE and full 3D simulation. The excellent agreement clearly demonstrates the efficiency and effectiveness of the quasi-1D NPSE approach, although we do find that it always seems to give a slightly shorter oscillation period as compared to the "exact" result.

Before concluding, we hope to discuss the conditions under which our quasi-1D NPSE description is applicable. For a true 1D condensate which enters the Tonks gas regime [21], our result is obviously not applicable. In the derivations of the quasi-1D NPSE, we have assumed a weak time- and z -dependence of the transverse mode. This assumption is valid only for weak excitations of the condensate such that the excitation in the transverse direction is negligible. In other words, the wavelength of the excitation is longer than the transverse size of the condensate. Under this condition, the transverse mode is reduced to the ground state which is a Gaussian in the weakly interacting limit and a TF profile in the strongly interacting limit. For spin-1 condensates widely discussed now, either of ^{23}Na or ^{87}Rb atoms, the spin-dependent excitation is always weak since c_2 is two or three orders of magnitude smaller than c_0 . The wavelength of the spin wave is thus larger than the transverse size of the condensate for a cigar-shaped trap [4, 5, 6, 9, 10, 11]. Our resulting NPSE model can thus be directly applied. For a strongly excited system, one has to include the transverse motion, with a more general approach as developed by Kamchatnov and Shchesnovich in [22] and Salasnich et al. in [23].

In summary, we have extended the successful effective quasi-1D nonpolynomial Schrödinger equation (NPSE) for a single-component scalar condensate to a multi-component spin-1 condensate in a cigar-shaped trap. We have demonstrated its validity with a Gaussian ansatz for the transverse profile in the weak interaction regime and with a Thomas-Fermi (TF) ansatz in the strong interaction regime. We have further demonstrated its effectiveness with studies on both the static (ground state) and dynamic properties of a spin-1 ^{87}Rb condensate in a cigar-shaped harmonic trap. With the effective quasi-1D NPSE, simulations for out of equilibrium condensate dynamics become rather efficient, thus allowing detailed comparisons with the recently observed spatial-temporal dynamics.

This work is supported by the NSF.

-
- [1] A. D. Jackson, G. M. Kavoulakis, and C. J. Pethick, Phys. Rev. A 58, 2417 (1998); L. Salasnich, Phys. Rev. A 70, 053617 (2004); L. Salasnich, A. Parola, and L. Reatto, Phys. Rev. A 65, 043614 (2002).
 - [2] M. L. Chiofalo and M. P. Tosi, Phys. Lett. A 268, 406 (2000).
 - [3] F. Gebier, Europhys. Lett. 66, 771 (2004).
 - [4] C. J. Myatt et al., Phys. Rev. Lett. 78, 586 (1997); D. S. Hall et al., Phys. Rev. Lett. 81, 1539 (1998); D. S. Hall et al., Phys. Rev. Lett. 81, 1543 (1998).
 - [5] J. Stenger et al., Nature (London) 396, 345 (1998).
 - [6] D. M. Stamper-Kurn et al., Phys. Rev. Lett. 80, 2027 (1998).
 - [7] M. D. Barrett, J. A. Sauer, and M. S. Chapman, Phys. Rev. Lett. 87, 010404 (2001).
 - [8] M.-S. Chang et al., Phys. Rev. Lett. 92, 140403 (2004).
 - [9] Private communication with M.-S. Chang and M. S. Chapman.
 - [10] H. Schmalthann et al., Phys. Rev. Lett. 92, 040402 (2004); H. Schmalthann et al., Phys. Rev. A 70, 031602(R) (2004).
 - [11] T. Kuwamoto et al., Phys. Rev. A 69, 063604 (2004).
 - [12] T.-L. Ho, Phys. Rev. Lett. 81, 742 (1998); T. Ohmichi and K. Machida, J. Phys. Soc. Jpn. 67, 1822 (1998).
 - [13] C. K. Law, H. Pu, and N. P. Bigelow, Phys. Rev. Lett. 81, 5257 (1998).
 - [14] S. Yi et al., Phys. Rev. A 66, 011601(R) (2002).
 - [15] H. Pu et al., Phys. Rev. A 60, 1463 (1999).

- [16] H. Pu, S. Raghavan, and N. P. Bigelow, Phys. Rev. A 61, 023602 (2000).
- [17] W. Zhang, S. Yi, and L. You, New J. Phys. 5, 77 (2003).
- [18] J. Vanier and C. Audoin, The Quantum Physics of Atomic Frequency Standards (A. Hilger, Philadelphia, 1988).
- [19] E. G. M. van Kempen et al, Phys. Rev. Lett. 88, 093201 (2002).
- [20] W. X. Zhang, D. L. Zhou, M. -S. Chang, M. S. Chapman, and L. You, (submitted, 2004).
- [21] M. Olschani, Phys. Rev. Lett. 81, 938 (1998); A. G. Orlicz et al, Phys. Rev. Lett. 87, 130402 (2001).
- [22] A. M. Kamchatnov and V. S. Shchesnovich, Phys. Rev. A 70, 023604 (2004).
- [23] L. Salasnich, A. Parola, and L. Reatto, Phys. Rev. A 69, 045601 (2004).